Near-Infrared Electrochemiluminescence from S, N-Doped Carbon Dots and Their Application for Ultrasensitive DNA Detection

Ming Yang,[a] Siyu Wen,[b] Kang Shao,[b] Xiaofeng Hu*[c] and Jing Wang*[b]*

[a]Department of Gastroenterology, The First Affiliated Hospital, Zhejiang University School of Medicine, Hangzhou 310003, China.

[b]College of Chemical Engineering, Zhejiang University of Technology, Hangzhou, 310014, P.R. China. E-mail: sk1033@zjut.edu.cn; Jingw1986@zjut.edu.cn

[c]National Reference Laboratory for Agricultural Testing (Biotoxin), Key Laboratory of Detection for Mycotoxins, Ministry of Agriculture and Rural Affairs, Oil Crops Research Institute of Chinese Academy of Agricultural Sciences, Wuhan 430062, China. E-mail: huxiaofeng@caas.cn

Table of Contents

1. Materials

Chemicals and reagents. Ultrapure water was obtained from a Millipore Milli-Q system (resistivity >18 MΩ·cm). Deionized formamide and DNA sequences were procured from Sangon Biotech (Shanghai) Co., Ltd. Bismuth nitrate, oleic acid, oleylamine, sublimed sulfur, cyclohexane, Tween-20, sodium borohydride, potassium persulfate, 6-mercapto-1-hexanol, N-hydroxythiosuccinimide, tri(2-carboxyethyl)phosphine hydrochloride, hydrogen peroxide solution, ascorbic acid, citric acid, sodium hypochlorite solution, and sodium citrate were acquired from Aladdin (Shanghai) Reagent Co., Ltd. Anhydrous ethanol, chloroauric acid, disodium hydrogen phosphate, and sodium dihydrogen phosphate were procured from China National Pharmaceutical Group Chemical Reagent Co., Ltd.

2. Experimental Section

2.1. Preparation of near-infrared carbon dots (NIR-CDs)

A 10 mL aqueous solution of glutathione formamide (3% w/v) was sealed in a 25 mL Teflon-lined stainless-steel autoclave and hydrothermally heated to and maintained at 160 °C for 1 h in a programmable muffle furnace. After natural cooling to ambient temperature (25 °C), the resulting dark brown solution was diluted fivefold with ultrapure water and subjected to dialysis purification using a regenerated cellulose dialysis membrane against deionized water for 7 days with frequent water changes (every 8 h). The dialyzed solution was then centrifuged at 12,000 rpm for 15 min and filtered through a 0.22 μm polyethersulfone membrane filter to remove aggregated particles. The purified NIR-CDs were concentrated via rotary evaporation and lyophilized to obtain a dark green powder, which was stored at -20 °C in amber vials until use.

2.2. Investigation of the ECL Properties of NIR-CDs

Initially, a 3 mm diameter glassy carbon electrode (GCE) was meticulously polished in succession with alumina powders of 1.00 μm, 0.30 μm, and 0.05 μm to yield a mirror-like surface finish. The electrode was then thoroughly rinsed with ultrapure water and subjected to ultrasonic cleaning in a 1:1 mixture of HNO_3 and H_2O. Following sonication, the electrode was extensively rinsed with copious amounts of water and dried under a stream of nitrogen. Next, 6 μL of NIR-CDs was precisely dispensed onto the electrode surface using a micropipette and allowed to air-dry at room temperature, resulting in a CDs-modified GCE. During the electrochemical and ECL

measurements, a three-electrode system was employed, comprising the CDs-modified GCE as the working electrode, a saturated Ag/AgCl electrode as the reference, and a platinum wire as the counter electrode. The supporting electrolyte consisted of a 0.1 M PB (pH 7.4) containing 0.1 M KCl.

2.3. Preparation of Bi_2S_3 and Bi_2S_3-Au NRs

A 2 mM solution of $Bi(NO_3)_3$ was dispersed in 10 mL of oleic acid and 10 mL of oleylamine within a 100 mL flask. The mixture was stirred and gradually heated to 170 °C under an argon atmosphere, maintaining this temperature for 40 minutes. Once the solution turned gray, 5 mL of an oleylamine solution containing 10 mM sulfur powder was swiftly injected. The reaction proceeded at 170 °C for an additional 10 minutes before being quenched by the rapid injection of 40 mL of chilled cyclohexane. The resultant product was collected by centrifugation at 10,000 rpm for 5 minutes, and the precipitate was washed three times with a 1:1 (v/v) mixture of hexane and ethanol. To render the synthesized Bi_2S_3 nanorods water-dispersible, Tween 20 was employed as a surface functionalizing agent. Specifically, 500 μL of Tween 20 was added to 50 mL of chloroform containing 50 mg of Bi_2S_3 nanorods, followed by stirring at ambient temperature for 2 hours. Subsequently, 50 mL of deionized water was introduced, and the mixture was stirred in a 50 °C water bath to facilitate the evaporation of chloroform. The Tween 20-functionalized Bi_2S_3 nanorods were then harvested by centrifugation and washed thoroughly with water three times.

Thereafter, 50 mg of the functionalized Bi_2S_3 nanorods were redispersed in water, and 200 μL of an aqueous $HAuCl_4$ solution (48.56 mM) was added. The mixture was stirred for 4 hours to allow for gold ion adsorption. Finally, 120 μL of a freshly prepared 100 mM $NaBH_4$ aqueous solution was introduced to reduce Au^{3+} to elemental gold. The resulting Bi_2S_3–Au nanorods were isolated by centrifugation and rinsed with deionized water three times.

2.4. Preparation of DNA tetrahedron nanostructure (DTNs)

DTNs were fabricated via a streamlined annealing process employing a one-pot incubation technique. Initially, four custom-designed single-stranded DNAs were diluted in a 20 mM PBS buffer (pH 7.4) containing 5.0 mM Mg^{2+} to a uniform final concentration of 5 μM. The strands were then combined in equimolar proportions, and the mixture was heated to 95 °C for 5 minutes before being gradually cooled to ambient temperature overnight to facilitate the formation of stable

DTNs. Finally, the assembled DTNs, featuring one amino group at the apex and three sulfhydryl groups at the remaining vertices, were stored at 4 °C for subsequent use.

Table S1. List of DNA Sequences Employed in the Experiment

Name	Sequences (5′ to 3′)
S1	NH_2- ACATTCCTAAGTCTGAATTCCTGGAGATACATGGCATTATTACAGCT TGCTACACGCCCTATTAGAAGGTCCGATTGAAGAGCCGTAG
S2	HS- TATCAGCAGGCAGTTGACGCGACAGTCGTTCAAGCCTTTCGGACCTT CTAATAGGGCGTGTAGCAAGCTGTAATTTATGCGAGGGTCCAATACT CTGTTCCGGGTGTGGCAT
S3	HS- GGCTTGAACGACTGTCGCGTCAACTGCCTGCTGATATTACGACACTA CGTAACGGTCGAGGACTGCTCCGCTGATTACTGCGGACACCGTAGCG ATCCGCCTACGGCTCTTC
S4	HS- TGCCATGTATCTCCAGGAATTCAGACTTAGGAATGTTTTCAGCGGAG CAGTCCTCGACCGTTACGTAGTGTCGTTTATGCCACACCCGGAACAG AGTATTGGACCCTCGCAT
Target DNA	GCGGATCGCTACGGTGTCCGCAGT

2.5. Construction of the ECL sensor

Fig. 3A delineates the fabrication process of the ECL sensor. Prior to each measurement, the GCE was methodically polished using sequential alumina slurries of 1 μm, 0.3 μm, and 0.05 μm particle sizes, then subjected to ultrasonic cleaning in a 1:1 (v/v) blend of nitric acid and water for 40 seconds each, and thoroughly rinsed with distilled water. The cleansed electrode was dried at ambient temperature before dispensing 6 μL of the Bi_2S_3–Au nanorod mixture centrally onto the GCE, where it was left to dry at room temperature for over three hours. The modified electrode was then rinsed in PBST and immersed in 20 μL of the pretreated DTNs solution, followed by an overnight incubation at 4 °C. Subsequently, after another PBST rinse, the electrode was immersed in 20 μL of a 6-mercapto-1-hexanol (MCH) solution for 15 minutes, rinsed again, and finally dipped in 10 μL of the pretreated DTNs solution with an overnight incubation at 4 °C.

2.6. Detection of target DNA

During the ECL measurements, a three-electrode configuration was employed, consisting of a GCE as the working electrode, a saturated Ag/AgCl electrode as the reference electrode, and a platinum wire as the counter electrode. The electrolyte comprised a 0.1 M PB solution (pH 7.4)

containing 0.1 M KCl. A scanning voltage from –1.3 to 0 V was applied at a rate of 0.30 $V \cdot s^{-1}$, and the photomultiplier tube was set to 700 V.

Initially, the modified electrode underwent ECL testing to record the corresponding luminescence intensity. Thereafter, the target DNA was serially diluted in a phosphate buffer solution supplemented with Mg^{2+} to achieve varying concentrations. Upon completion of the preliminary tests, the electrode was individually immersed in 100 μL aliquots of these target DNA solutions and incubated at room temperature for 1.5 hours. The electrode was then sequentially rinsed with PBST and deionized water prior to undergoing further ECL detection.

3. Measurement

Absorption spectra were acquired using a Persee TU-1900 UV-vis spectrometer, while fluorescence spectra were recorded with a Hitachi F-2700 spectrofluorometer under 365 nm excitation. Transmission electron microscopy (TEM) was conducted on an FEI Tecnai G2 F30 electron microscope operating at 200 kV. Dynamic light scattering (DLS) and zeta potential measurements were performed with a Malvern Zetasizer Nano-ZS90. X-ray diffraction (XRD) analysis was executed on a Dutch PNAlytical X'Pert PRO diffractometer operating at 40 kV and 40 mA. Fourier-transform infrared spectroscopy (FTIR) were obtained using a Thermo Nicolet 6700 Fourier-transform infrared microspectrometer. ECL analyses were carried out on an MPI-EII electrochemiluminescence detection system. ECL spectrum was recorded during potential scanning using a custom-built ECL system comprising an Autolab PGSTAT302N workstation (Metrohm, The Netherlands) and a QEpro spectrophotometer. A homemade Teflon cell, equipped with a circular quartz window, optical fiber, and collimating lens, was employed. The integration time for each spectrum was set to 0.3 s, with a scan rate of 0.1 V s^{-1}. X-ray photoelectron spectroscopy (XPS) was recorded on a Japanese Shimadzu-Kratos Kratos AXIS Ultra DLD spectrometer.

4. Supporting Figures and Tables

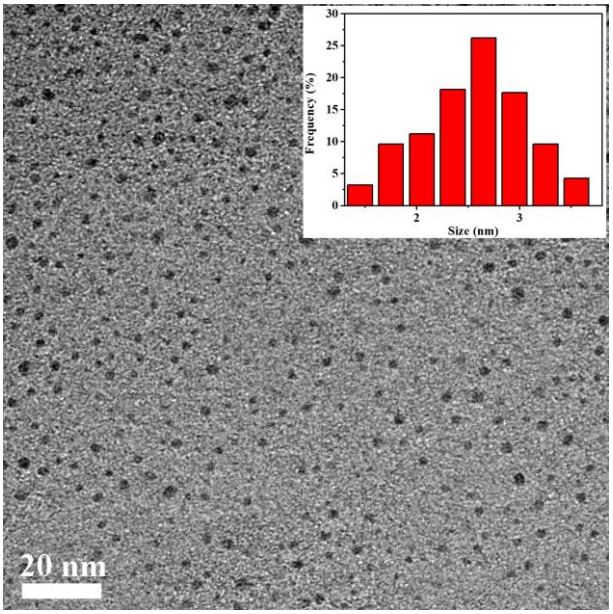

Fig. S1. TEM image of NIR-CDs, inset shows the corresponding particle size distribution.

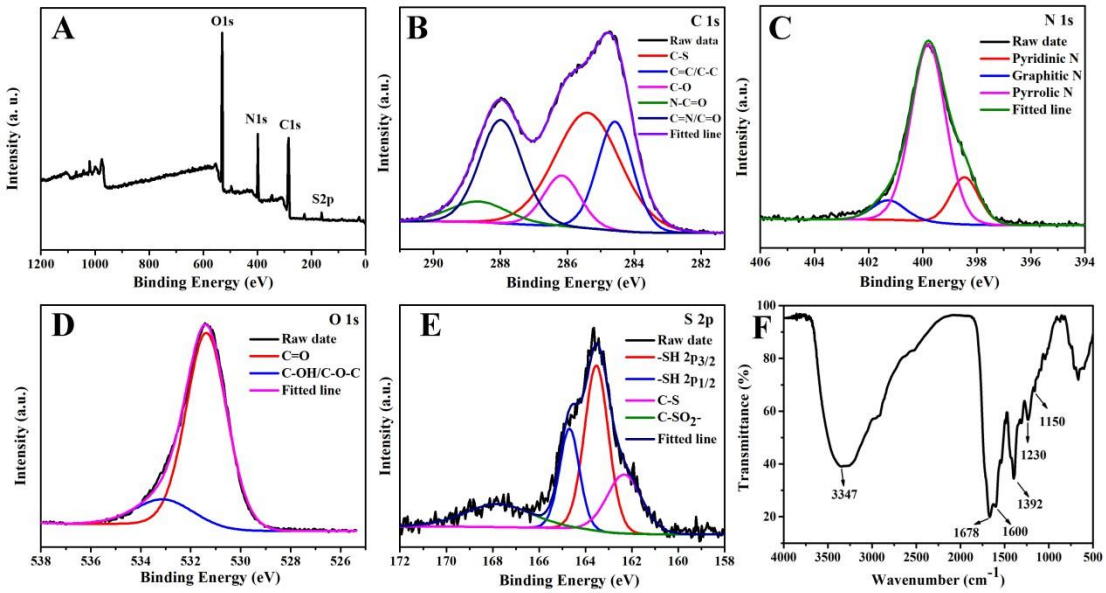

Fig. S2. (A) XPS survey spectrum of the NIR-CDs. High-resolution XPS spectra of (B) C 1s, (C) N 1s, (D) O 1s, and (E) S 2p regions. (F) FTIR spectrum of the NIR-CDs.

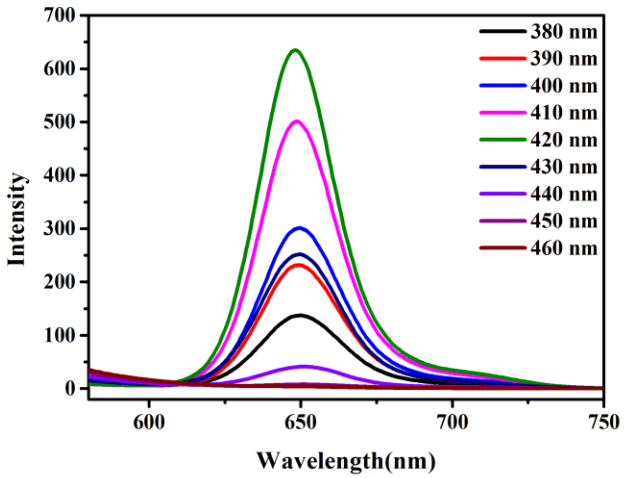

Fig. S3. Fluorescence spectra of NIR-CDs tested under different excitation wavelengths. The fluorescence spectra of the NIR-CDs were recorded under excitation wavelengths ranging from 380 nm to 460 nm. Despite this variation, the emission maximum remains steadfastly at ~650 nm, confirming that their near-infrared fluorescence is excitation-independent and not attributable to surface defects. Notably, the CDs exhibit peak fluorescence intensity upon 420 nm excitation.

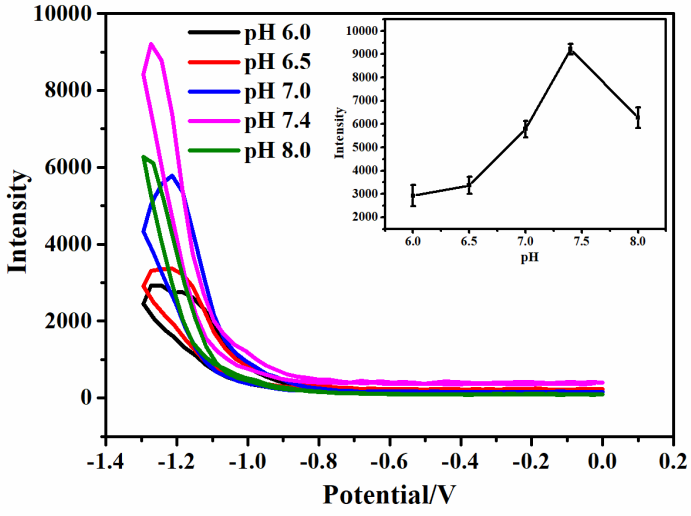

Fig. S4. Effect of pH on the ECL intensity of NIR-CDs/GCE. The ECL intensity increased with rising pH before subsequently diminishing, ultimately reaching its peak at pH 7.4. Therefore, the optimal pH for the electrolyte solution was determined to be 7.4.

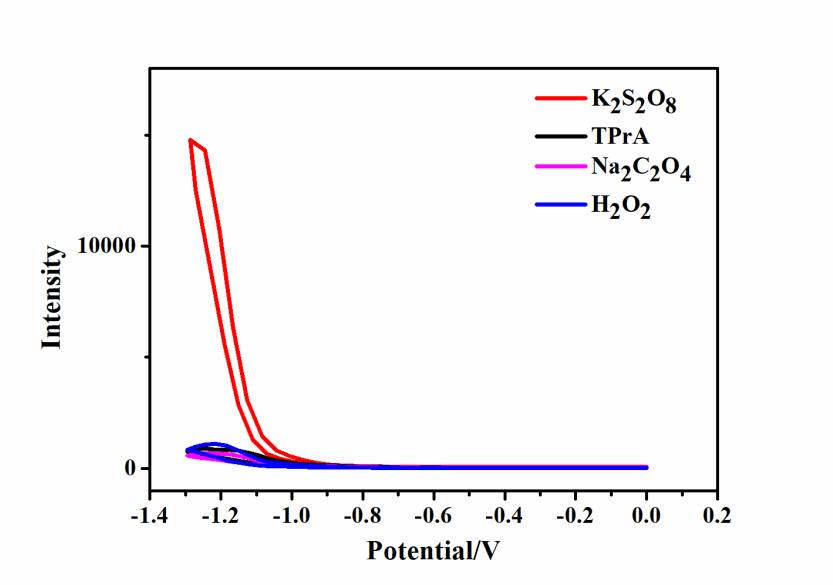

Fig. S5. Effect of co-reactants on the ECL intensity of NIR-CDs/GCE. When $K_2S_2O_8$ solution served as the co-reactant, the system exhibited its maximum ECL intensity, whereas nearly no ECL signal was produced under other co-reactant conditions; therefore, $K_2S_2O_8$ was ultimately selected as the co-reactant for this experiment.

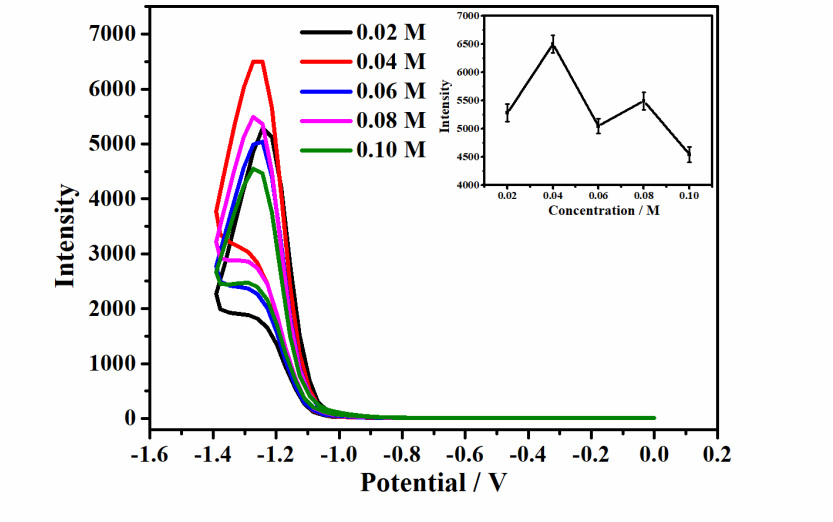

Fig. S6. Effect of the concentration of $K_2S_2O_8$ on the ECL intensity of NIR-CDs/GCE. With increasing concentrations of $K_2S_2O_8$, the ECL intensity initially escalated before diminishing. At a concentration of 0.04 M, the intensity achieved its zenith, thereby establishing 0.04 M as the optimum co-reactant concentration for the system.

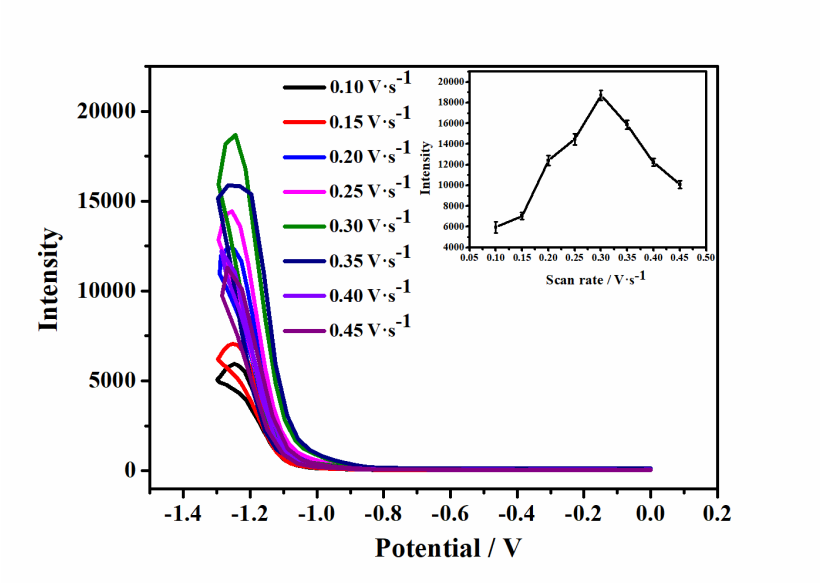

Fig. S7. Effect of scan rate on the ECL intensity of NIR-CDs/GCE. When the scanning rate reached 0.30 $V \cdot s^{-1}$, the intensity of the CDs peaked, thereby establishing 0.30 $V \cdot s^{-1}$ as the optimal scanning rate.

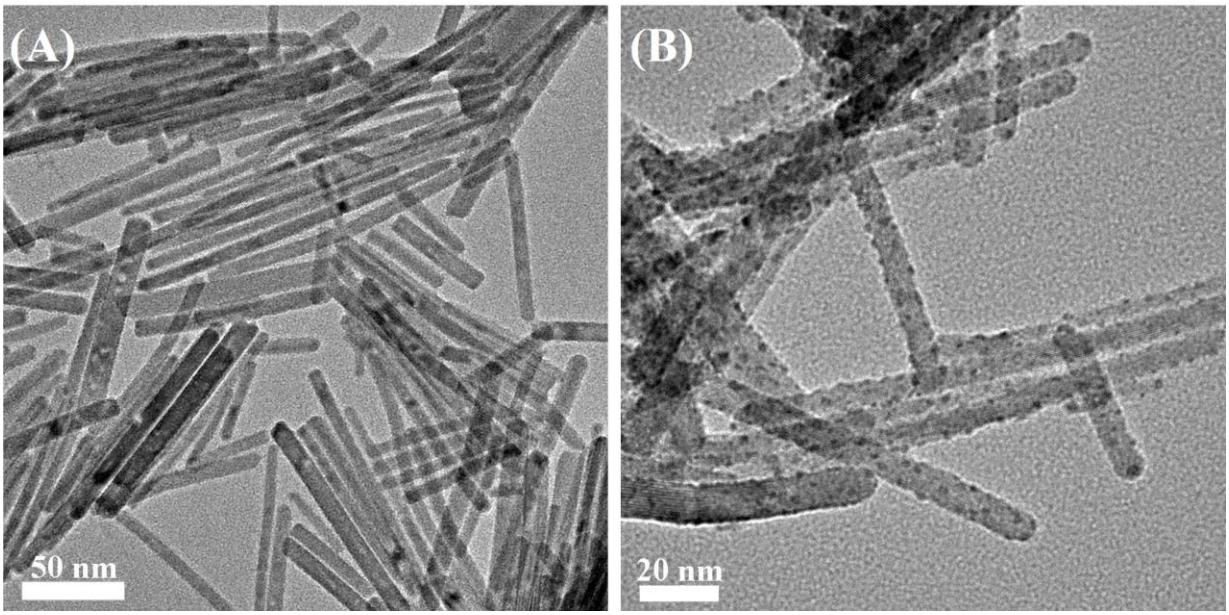

Fig. S8. TEM images of (A) Bi_2S_3 and (B) Bi_2S_3-Au NRs

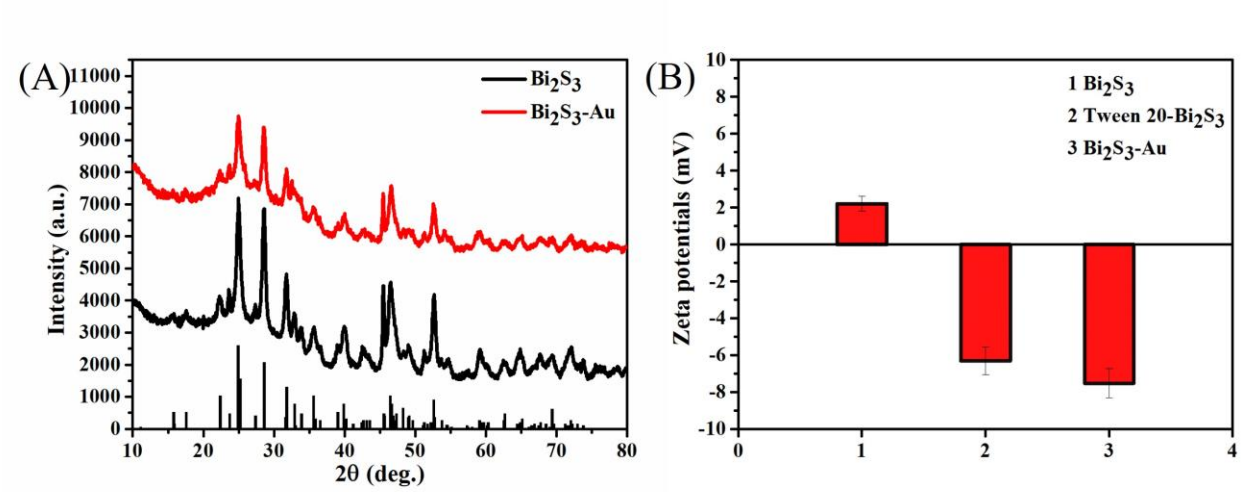

Fig. S9. (A) XRD patterns of Bi_2S_3 and Bi_2S_3-Au NRs. (B) Zeta potential distributions of Bi_2S_3, Tween 20 modified Bi_2S_3 (Tween 20-Bi_2S_3), and Bi_2S_3-Au NRs.

As illustrated in **Fig. S9A**, the XRD patterns of Bi_2S_3 and Bi_2S_3-Au nanorods were juxtaposed with the simulated standard pattern of Bi_2S_3 nanorods (JCPDS: 17-0320), thereby confirming the successful synthesis of Bi_2S_3-Au NRs and demonstrating that the deposition of AuNPs on the Bi_2S_3 surface does not impede its crystalline growth. The Zeta potentials of the products at each stage were subsequently measured. As shown in **Fig. S9B**, the as-synthesized Bi_2S_3 nanorods exhibited a positive Zeta potential, which inverted to negative upon functionalization—an effect likely due to the abundance of carboxyl or hydroxyl groups on the Bi_2S_3 surface. Moreover, the further negative shift in the Zeta potential of the Bi_2S_3-Au nanorods indicates the successful growth of Au on the surface of the Bi_2S_3 nanorods.

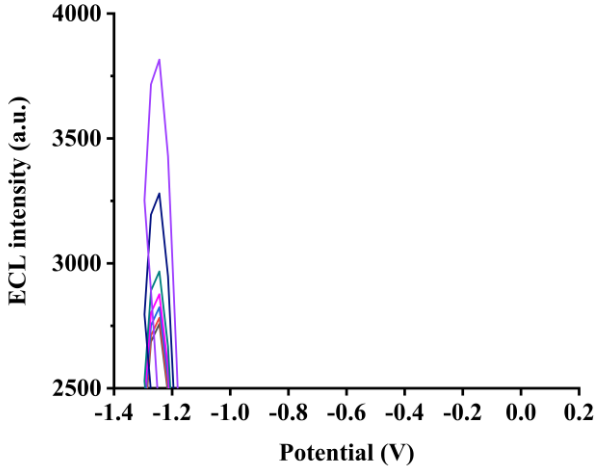

Fig. S10. The enlarged ECL-potential curves under varying target DNA concentrations.